Pacific Graphics (2020)
E. Eisemann, A. Jacobson, and F.-L. Zhang (Editors)

Short Paper

Monocular 3D Fluid Volume Reconstruction Based on a Multilayer External Force Guiding Model

Zhiyuan Su[*,1], Xiaoying Nie[*,1], Xukun Shen[1,2], and Yong Hu[†,2,1]

[*] joint first authors
[1]State Key Laboratory of Virtual Reality Technology and Systems, Beihang University
[2]School of New Media Art and Design, Beihang University

Abstract

In this paper, we present a monocular 3D fluid volume reconstruction technique that can alleviate challenging parameter tuning while vividly reproducing the inflow and outflow of the video scene. To reconstruct the geometric appearance and 3D motion of the fluid in the video, we propose a multilayer external force guiding model that formulates the effect of target particles on fluid particles. This multilayer model makes the whole 3D fluid volume subject to the shape and motion of the water captured by the input video, so we can avoid tedious and laborious parameter tuning and easily balance the smoothness of the fluid volume and the details of the water surface. Besides, for the inflow and outflow of the 3D fluid volume, we construct a generation and extinction model to add or delete fluid particles according to the 3D velocity field of target particles calculated by a hybrid model of coupling SfS with optical flow. Experiments show that our method compares favorably to the state-of-the-art in terms of reconstruction quality, and is more general to the real-captured fluid. Furthermore, the reconstructed 3D fluid volume can be effectively applied to any desired new scenario.

CCS Concepts

• ***Computing methodologies*** → ***Physical simulation; Modeling methodologies;***

1. Introduction

Monocular fluid reconstruction is especially challenging due to the water's complex topological variation and frequent occlusions [WLZ*09, TZG*18, TLY20]. The traditional physically-based simulation methods [MCG03, FM96, Sta99] suffer from high time consumption, challengeable and tedious parameter tuning to generate desirable fluid behaviors captured from the real world [TL19]. The Shape from Shading (SfS) methods [ZTCS99, TS94, DWSK18] can be utilized to reconstruct the 3D surface of the water from its 2D intensity image, but it is incapable of recovering the internal volume and the physical property.

The latest research [NHSS19] illustrated the power of the external force scheme, which can solve the problem of 3D fluid reconstruction from a monocular video by constructing the mapping between SfS method and SPH model. The external force scheme formulates the guidance of the input monocular video to a 3D fluid volume and makes it possible to recover the water surface and volume. However, due to the large height difference of the reconstructed water surface by SfS, it is difficult to maintain the fluid surface details while eliminating the fluid volume holes. Consequently, to obtain satisfactory visual results, tedious and laborious trial-and-error parameter manually tuning steps are inevitable. In practice, the external force scheme requires high time overhead, because besides parameter turning, fluid reconstruction can also take several hours or more to check intermediate results.

In this paper, we significantly improve Nie's [NHSS19] work and propose a multilayer external force guiding model that commendably compensates for the imperfection in height field and weakens the influence of parameter values on the reconstruction results. We follow the definition of fluid particles and target particles from [NHSS19] and combine SfS with optical flow to estimate the position and velocity field of target particles, and further interpolate the multilayer target particles with geometric and physical properties. To be highly consistent with the fluid scene in the input video, we revise the initialization of fluid particles in [NHSS19], and propose a generation and extinction model of fluid particles, whose inflow and outflow are embedded into the SPH model to form a stable fluid with open boundaries. Our work develops a low-consumption and easy-to-use reconstruction framework to intuitively and efficiently reconstruct the fluid from real world video. Main contributions of this paper are:

- We propose **a multilayer external force guiding model** to reconstruct a 3D fluid volume with surface details from a monocular video. We show that the advantage of the "multilayer" frame-

† Corresponding author: huyong@buaa.edu.cn

DOI: 10.2312/pg.20201225

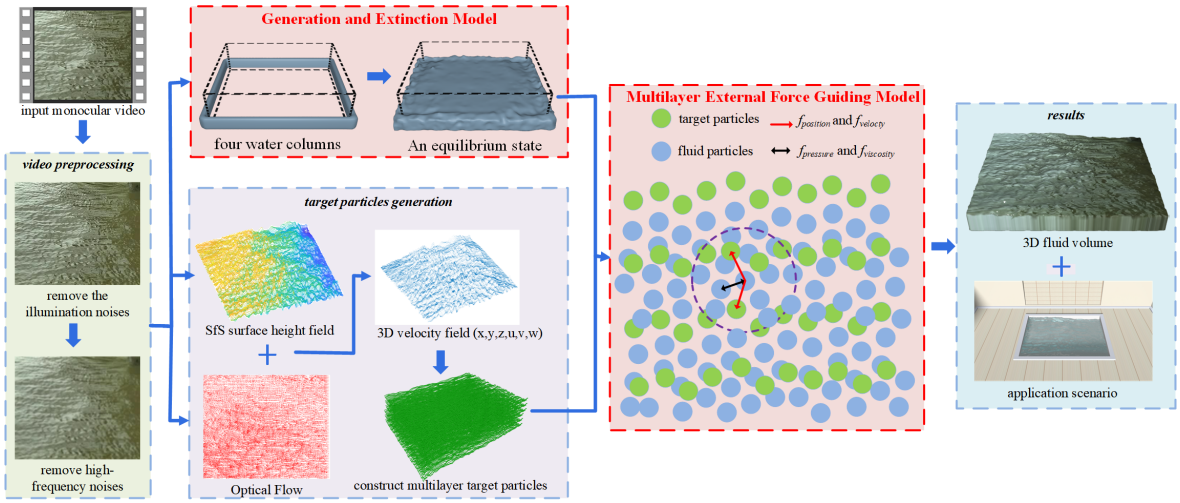

Figure 1: *An overview of our method. The input is a monocular video, and the output is a 3D fluid volume. Based on the denoising video, we construct fluid particles with generation and extinction features, and generate multilayer target particles with the 3D position data and velocity field. Under the action of the multilayer external force guiding model, the reconstructed 3D fluid volume can represent the geometric appearance and 3D motion of the video to the life, and it can be effectively applied to any desired new scenario.*

work based on the SPH model is that the guiding strategy can be significantly simplified since there is no need to manually tune parameters through laborious and tedious trial-and-error processes.

- We introduce **a generation and extinction model of fluid particles** to reproduce inflow and outflow behaviors of the fluid in the video, preserve the observed fluid properties in the real world. We believe that this is an important key step towards bridging the gap between the reconstructed result and the input video.

2. Overview

Our goal is to reconstruct a 3D fluid volume to simulate fluid behaviors as close as possible to the water phenomena captured from the monocular video. Figure 1 illustrates our fluid reconstruction framework. Our framework consists of two stages: the particles preparation stage and the external force guidance stage. In the particles preparation stage, our framework takes a large-scale and opaque water video as input. Firstly, we preprocess the video by removing the illumination noises and high-frequency noises. Then we construct multilayer target particles with positional data and the 3D velocity field using SfS and optical flow method. Simultaneously, we initialize the fluid particles based on the generation and extinction model. The external force guidance stage is an iterative process. Firstly, based on SPH model, we first perform fluid simulation by calculating the internal forces between fluid particles. Next, we employ target particles to guide fluid particles based on the multilayer external force guiding model to vividly reproduce the geometric appearance and motion field of the input video. Our framework iteratively adds or deletes fluid particles based on the generation and extinction model to realize the inflow and outflow of the 3D fluid volume.

3. Fluid Reconstruction Method

Both of the techniques we describe here together constitute a method for reconstructing the appearance and behavior of 3D fluid volume. By developing a multilayer external force guiding model for the SPH method and proposing a generation and extinction model for fluid particles, we can easily recover various water scenes from monocular videos.

3.1. The Multilayer External Force Guiding Model

In [NHSS19], target particles were placed directly above the 3D fluid volume as shown in Figure 2(a), and then the position traction force and the velocity guidance force were applied to their neighboring fluid particles. The overall relative height difference ΔH of target particles and fluid particles plays an essential role on the visual results simulated by SPH. Smaller ΔH results in some holes in the 3D fluid volume, and larger ΔH results in too flat surface and misses surface details. Meanwhile, ΔH value is also related to the smooth radius h, the external force weight coefficients w_a and w_V,

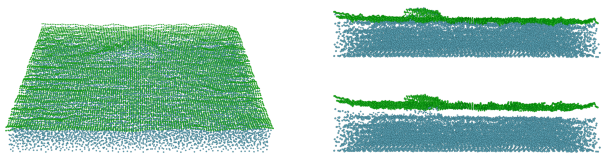

(a) Target particles were placed directly above the 3D fluid volume

(b) The top sub-figure shows the smaller ΔH, and the bottom sub-figure shows the larger ΔH.

Figure 2: *[NHSS19]'s target particles (green points), fluid particles (blue points).*

the time step Δt and other physical parameters, which makes the parameter tuning process extremely time-consuming.

Therefore, we design a multilayer external force guiding model so that both of fluid particles on the surface and inside of the 3D fluid volume are guided by target particles. We borrow some fundamental concepts from [NHSS19] to intuitively and efficiently symbolize our model through two kinds of particles, a set of fluid particles $\mathcal{I} = \{i \in \mathcal{I} \mid i = 1,2,3,\cdots,n_i\}$ and a set of target particles $\mathcal{G} = \{g \in \mathcal{G} \mid g = 1,2,3,\cdots,n_g\}$, and two external forces, the position traction force f_p and the velocity guidance force f_V. Fluid particles $\mathcal{I}$ describe a 3D fluid volume by sampling the continum and target particles $\mathcal{G}$ are generated from input video to drive fluid particles to achieve the desired behavior. Here n_i and n_g denote the number of fluid particles and target particles respectively. The position traction force f_p is determined by the distance r_{ig} between a fluid particle i and a target particle g, and its connotation is that the target particle g acts as a local magnet to attract nearby fluid particles. The velocity guidance force f_V is dependent on the velocity difference V_{ig} between a fluid particle i and a target particle g, and its motivation originates from which the motion of the target particle g is similar to wind forces to transport fluid particles along its moving path [MM13].

As in [NHSS19, LPS*13], we sample the height field of water surface acquired by SfS to produce target particles. Thus, the position information of each target particle is obtained and expressed as $r_g(x,y,z)$. And we use optical flow [LPS*13] to estimate the velocity $V_g(u,v,w)$ of the target particle. As shown in Figure 3, these target particles are interpolated in the vertical direction as a whole without changing of the horizontal relative position and velocity field. The interpolation step size of multilayer target particles is determined by the smooth radius h of fluid particles, which also determines the spacing of fluid particles in the SPH model. Accordingly, the target particles maintain spatial consistency with the fluid particles.

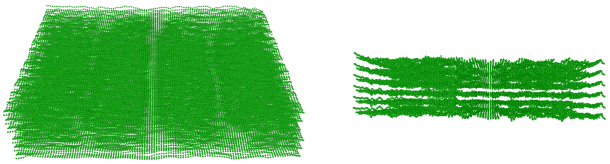

Figure 3: *The target particles of our multilayer external force guiding model.*

Accompanied by the generation of multilayer target particles, the 3D fluid volume is guided by multilayer external forces. The external forces are computed as follows:

$$f_p(i) = w_a \sum_{g=1}^{c \times n_g} \alpha_g \frac{r_g - r_i}{||r_g - r_i||} W(r_{gi}, h) \tag{1}$$

$$\alpha_g = 1 - min(1, \sum_{i=1}^{n_i} \frac{m_i}{\rho_i} W(r_{gi}, h)) \tag{2}$$

$$f_V(i) = w_V \sum_{g=1}^{c \times n_g} (V_g - V_i) W(r_{gi}, h) \tag{3}$$

where α_g scales down the position traction force when the influence region of the target particle is already sufficiently covered with fluid. w_a and w_V are global constants that define the strength of the position traction force and velocity guidance force respectively. $r_{gi} = ||r_g - r_i||$ denotes Euclidean distance between the target particle g and the fluid particle i. V_i, r_i, ρ_i and m_i denote the velocity, position, density, mass of the fluid particle i, respectively. h denotes the smooth radius, and W denotes the target particle kernel function. Here we use a normalized spline kernel [MCG03, TKPR09] to be the target particle kernel function as the same as the density approximation. The number of multilayer target particles $(g = 1,2,3,\cdots,n_g,\cdots,2 \times n_g,\cdots,c \times n_g)$ is an integer multiple (i.e. c) of the number of a single-layer target particles $(g = 1,2,3,\cdots,n_g)$.

3.2. The Generation and Extinction Model

Nie et. al [NHSS19] generated fluid particles according to the aspect ratio of video frames. These fluid particles move in a fixed bounding box to produce surface appearance similar to target particles. But for the water example with obvious inflow and outflow, a fixed number of fluid particles cannot accurately track the flow movement at a fixed boundary. To overcome these problems, we propose a generation and extinction model to add or delete fluid particles in the reconstruction scene to better approximate the dynamic variation of the water in the video.

As shown in Figure 4(a), our scene is a bounding box whose size is proportional to the height and width of the input video frame, and only the bottom is fixed and the other five sides are open. Clinging close to front, back, left, right outer edges of the bounding box, we place four water slices whose size are set as the same as the size of the corresponding side to ensure that the generation of particles in the four directions is evenly and balanced to avoid unexpected turmoil of the 3D fluid volume. Throughout the fluid reconstruction, four water slices move under the action of gravity. We add the particles entering the bounding box into the 3D fluid volume and treat this process as the generation of fluid particles, that is the inflow phenomenon of fluid. Likewise, we remove the particles flow out the bounding box boundary from the 3D fluid volume and treat this process as the extinction of fluid particles, that is the outflow phenomenon of fluid.

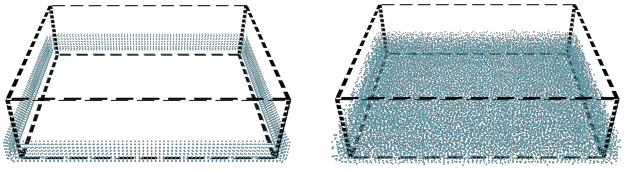

(a) four water slices (blue points) outside the open bounding box (black dashed frame)

(b) an equilibrium state of the 3D fluid volume (blue points)

Figure 4: *The generation and extinction model of fluid particles.*

In the initialization stage of the 3D fluid volume, we drive the particles flowing into the bounding box to reach an equilibrium state (Figure 4(b)), e.i. relative stillness only under the action of

gravity and internal forces in SPH. This can suppress the interference of water columns falling, splashing, collision, etc., to the multilayer external force guiding model in the stage of fluid reconstruction.

4. Result

We tested our method on a PC with a 3.6 GHz Intel Core i7-7700 CPU and an NVIDIA TITAN X (Pascal) graphics card with 12 GB memory. Our iterative reconstruction process is implemented with C++ and CUDA. Houdini renderer is utilized to render our reconstructed fluid results. In the following, we first verify the reliability of our reconstruction method with experiments on the synthetic data, then present comparisons to state-of-the-art works. Subsequently, we evaluate our model with fluid videos in the public Dyntex dataset [PFH10]. Finally, we provide some application scenarios of the reconstructed 3D fluid volume.

4.1. Validation with Synthetic Data

To verify our model, we generated a video using our SPH fluid solver and used this synthetic data as input. The purpose of this experiment is to validate that our 3D fluid volume can reproduce the geometric appearance and 3D motion field. As shown in Figure 5, the first column shows the ground truth and the second column shows the reconstructed 3D fluid volume. The first and second rows show comparisons in different render views. The third column shows the residual depth of this frame from a top view. The visual differences between the ground truth and the reconstructed result are not significant. For each frame, we evaluate the depth error [NHSS19] of the ground truth and the reconstruction results. Quantitative analysis of the reconstructed errors is given in Table 1. The maximum standard deviation of depth is 0.021. This shows that the deviation from the reconstruction results is slight and acceptable.

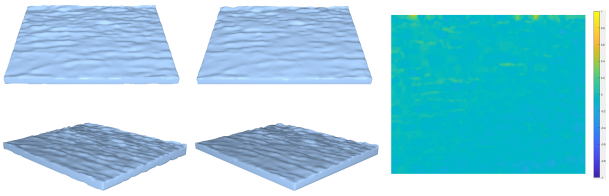

Figure 5: *Validation with ground truth. Multiple perspectives comparisons between synthetic Data (first column) and our reconstructed 3D fluid volume (second column). The third column is the residual depth.*

4.2. Comparative experiments to verify the innovation points

Fluid videos are selected from the public Dyntex dataset, with the length of 10 seconds (250 frames), and the resolution of 352×288. The overall computation time depends on the video resolution, the number of video frames, and the experimental environments. Under these identical conditions, we compare with the paper [NHSS19]. To reconstruct a same 3D fluid volume, Nie et al. [NHSS19] spent an average of 291.1 seconds, while we took an average of 220.3 seconds. Although our multilayer external force guiding model requires more target particles, our generation and extinction model reduces the number of fluid particles, thus reducing time consumption.

Table 1: *Statistics result of the depth errors*

Frame Number	Error	Frame Number	Error	Frame Number	Error
1	0.0052	61	0.0032	121	0.0036
11	0.0026	71	0.003	141	0.0018
21	0.0026	81	0.0023	151	0.002
31	0.0067	91	0.0039	161	0.0035
41	0.0074	101	0.0027	171	0.0023
51	0.0022	111	0.0083	181	0.021

Our multilayer external force guiding model solves the difficulty of balancing holes and details. This is because our model expands the influence range of external forces so that the whole 3D fluid volume is uniformly guided. The advantage of our model makes it easy to determine an appropriate overall relative height ΔH of target particles and fluid particles. Even ΔH is too large, the surface of 3D fluid volume can also be correctly guided, this is because multilayer target particles are generated downward from the surface layer for external force guidance. Figure 6(a) and Figure 6(b) respectively show Nie et al.'s reconstruction results in the same rendering environment, where $\Delta H = 0$ and $\Delta H = -0.015$ respectively. As shown in Figure 6(a), the reconstructed surface is very flat. This is due to the excessive value of ΔH, which results in a significant portion of the surface fluid particles not being guided by sufficiently large external forces. There are some obvious holes on the surface in Figure 6(b). This is because target particles only guide the surface fluid particles, but have very weak influence on the internal fluid particles. This leads to the inner hollow of the protruding surface and results in the instability of the geometric details of the fluid surface. Figure 6(c) shows our reconstruction result. Because of the multilayer external forces, the whole 3D fluid volume is guided to preserve rich details and maintain the smooth of 3D volume.

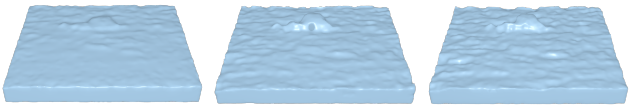

(a) $\Delta H = 0$ (b) $\Delta H = -0.015$ (c) ours

Figure 6: *Comparison between Nie et al's (a, b) and ours. (a) The reconstructed result is too smooth and missing surface details because the ΔH value is large. (b) There are some holes in the 3D fluid volume because the ΔH value is small.*

Furthermore, we designed an experiment to verify the effectiveness of our generation and extinction model. In the initialization stage of the 3D fluid volume, a ball drops into the still water. Then the particles of the ball move respectively under the action of Nie et al.'s [NHSS19] model and our model. Figure 7 shows the four

states of the ball's falling process, falling into the 3D fluid volume, guiding movement and the end of reconstruction. The first row shows the results of Nie et al. We can see that the number of ball particles has not changed, and their horizontal positions have changed a little. The second row shows our results. The number of ball particles has an obvious decrease, and these particles have a distinct horizontal motion. Our result vividly reproduces the inflow and outflow of the video scene. This significant promotion owes to our generation and extinction model and the guidance of target particles' 3D velocity field.

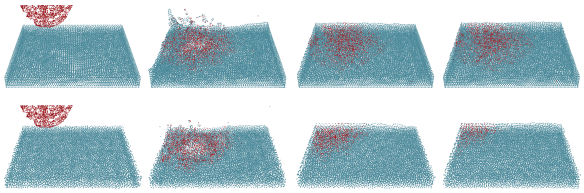

Figure 7: *The verified experiment of the generation and extinction model. The first row shows the results of Nie et al. and the second row shows our results. The columns show the four states of the ball particles (red points) at the corresponding moment. The blue points denote the 3D fluid volume.*

4.3. Reconstruction from Real Video

Each video in the Dyntex dataset is captured in the real world. Owing to the influence of weather, illumination and reflective characteristics of water surface, the illumination distribution in the obtained fluid video is not uniform. And there are also high-frequency phenomena such as foam, splash or spray in video frames, which cause a large amount of noises in the acquired height field and greatly reduce the accuracy of the fluid reconstruction. We use gamma function [WYZ*17,HWY*19] and Low-Pass Gaussian Filtering [QRL*12,GLML20] to remove illumination noises and high-frequency noises in the video frame.

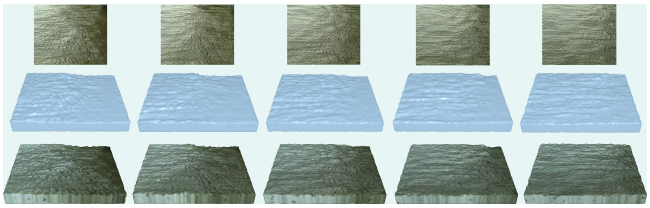

Figure 8: *3D fluid volumes of Gentlewaves. Given five frames of the monocular video (the first row), our method generates a series of opaque 3D fluid volumes (the second row) to better illustrate the surface details, and renders them with the same texture (the third row) as the input video to show 3D motion field.*

We design two sets of experiments: gentle motion (Figure 8) and complex motion (Figure 9). First, we use pure SPH simulation to initialize the fluid particles. We set the time step to 0.01 ($\Delta t = 0.01$). Based on the generation and extinction model, it takes about 150 iterations to obtain a relatively still 3D fluid volume. The time step of the reconstruction process is 0.002 ($\Delta t = 0.002$). We adopt an adaptive time step selection strategy. A large time step is used to accelerate the simulation of the initialization phase which does not require high precision, and a small time step is used to improve the accuracy of reconstruction. For each frame, target particles guide 20 iterations of the fluid particles. This can maintain time consistency with the frame rate of the video. For all videos, we interpolate three layers of target particles. The spacing between layers is half of the smooth radius ($0.5h$). Besides, we adopt $w_a = 0.018/h$, $w_V = 0.005/h$ to define the weight of the position traction force and the velocity guidance force respectively. Our results (Figure 8 and 9) show that our algorithm is capable of realistically reconstructing several large-scale liquid phenomena.

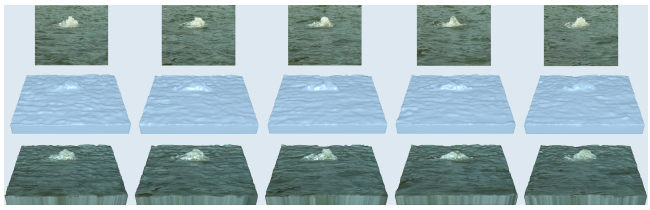

Figure 9: *3D fluid volumes of Fountain. From the input video (the first row), two rendering methods (the second and third rows) for five frames (each column) show the reconstructed geometric appearance and 3D motion.*

4.4. Application Scenarios

It is worth mentioning that the reconstructed 3D fluid volume can be flexibly utilized, e.g., for re-simulation, domain modification or guiding purposes, and has wide applications in films, cartoons, computer games, AR and so on. Figure 10 shows some application examples such as the fabulous indoor or square Fountain (Figure 10(a)), the stunning shopping mall Gentlewaves (Figure 10(b)). Slightwaves of beach (Figure 10(c)) in the summer let us feel comfortable and cozy. The 3D fluid volume of the Surge blends and harmonizes with bridge (Figure 10(d)) and presents us with a fast-flowing and treacherous river.

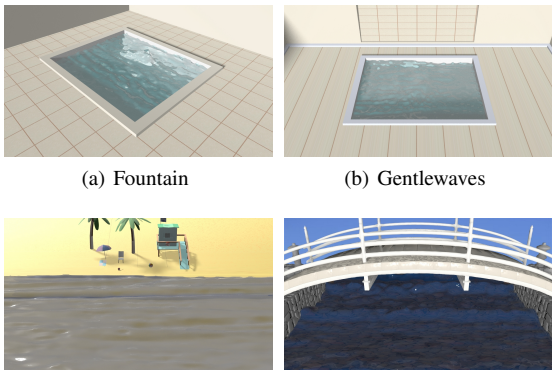

(a) Fountain (b) Gentlewaves

(c) Slightwaves (d) Surge

Figure 10: *Application scenarios of the reconstructed results.*

5. Conclusion

We have presented perhaps the first approach that efficiently reconstructs 3D fluid volumes with rich surface details and no loopholes. Our framework takes the monocular fluid video as a reference to guide the 3D fluid volume simulation. To promote the guidance, we proposed a multilayer external force guiding model, which appends the position traction force and the velocity guidance force to SPH, avoiding trial-and-error parameter tuning step. Simultaneously, we simulated the inflow and outflow behavior of the 3D fluid volume based on the 3D velocity field of target particles and the generation and extinction model of fluid particles. We validated our reconstruction method with a range of synthetic and real videos and demonstrated that our model can efficiently generate fluid behaviors visually consistent to the video and the reconstructed 3D fluid volume can be effectively applied to any desired new scenario.

Our approach also has a few limitations, which can be addressed in the future work. We subtly set up the generation and extinction of fluid particles, but the addition and deletion of fluid particles inevitably led to boundary jitters of the 3D fluid volume. Further refinement of the generation and extinction model would be a promising future research direction. In addition, the input videos have no background, which weakens the universality of our reconstruction method. Thus, it would be necessary to explore some techniques to obtain meaningful and reliable fluid information from general videos available in public. We would also like to advocate seeking novel strategies for water surface reconstruction, such as investigating the machine learning approach [LMK*18, SLFC19] and advanced computer vision techniques to replace the SfS method that is limited by many assumptions.

Acknowledgement

This work is supported in part by National Key R&D Program of China (No.2017YFB1002702) and National Natural Science Foundation of China (U19A2063). The authors sincerely thank all the anonymous reviewers for their kind suggestions.

References

[DWSK18] DOU P., WU Y., SHAH S. K., KAKADIARIS I. A.: Monocular 3d facial shape reconstruction from a single 2d image with coupled-dictionary learning and sparse coding. *Pattern Recognit. 81* (2018), 515–527. 1

[FM96] FOSTER N., METAXAS D. N.: Realistic animation of liquids. *CVGIP Graph. Model. Image Process. 58*, 5 (1996), 471–483. 1

[GLML20] GUO X., LI Y., MA J., LING H.: Mutually guided image filtering. *IEEE Trans. Pattern Anal. Mach. Intell. 42*, 3 (2020), 694–707. 5

[HWY*19] HAN P., WANG D., YANG X., LIU Y., LI D., XU Z., WANG J.: An improved adaptive correction algorithm for non-uniform illumination panoramic image. In *2019 IEEE 2nd International Conference on Electronic Information and Communication Technology (ICEICT)* (2019), pp. 258–262. 5

[LMK*18] LI Z., MUREZ Z., KRIEGMAN D. J., RAMAMOORTHI R., CHANDRAKER M.: Learning to see through turbulent water. In *2018 IEEE Winter Conference on Applications of Computer Vision, WACV 2018, Lake Tahoe, NV, USA, March 12-15, 2018* (2018), IEEE Computer Society, pp. 512–520. 6

[LPS*13] LI C., PICKUP D., SAUNDERS T., COSKER D., MARSHALL A. D., HALL P. M., WILLIS P.: Water surface modeling from a single viewpoint video. *IEEE Trans. Vis. Comput. Graph. 19*, 7 (2013), 1242–1251. 3

[MCG03] MÜLLER M., CHARYPAR D., GROSS M. H.: Particle-based fluid simulation for interactive applications. In *Proceedings of the 2003 ACM SIGGRAPH/Eurographics Symposium on Computer Animation, San Diego, CA, USA, July 26-27, 2003* (2003), Parent R., Singh K., Breen D. E., Lin M. C., (Eds.), The Eurographics Association, pp. 154–159. 1, 3

[MM13] MADILL J., MOULD D.: Target particle control of smoke simulation. In *Graphics Interface 2013, GI '13, Regina, SK, Canada, May 29-31, 2013, Proceedings* (2013), pp. 125–132. 3

[NHSS19] NIE X., HU Y., SU Z., SHEN X.: External Forces Guided Fluid Surface and Volume Reconstruction from Monocular Video. In *Pacific Graphics Short Papers* (2019), Lee J., Theobalt C., Wetzstein G., (Eds.), The Eurographics Association. 1, 2, 3, 4

[PFH10] PÉTERI R., FAZEKAS S., HUISKES M. J.: Dyntex: A comprehensive database of dynamic textures. *Pattern Recognit. Lett. 31*, 12 (2010), 1627–1632. 4

[QRL*12] QU F., REN D., LIU X., JING Z., YAN L.: A face image illumination quality evaluation method based on gaussian low-pass filter. In *2nd IEEE International Conference on Cloud Computing and Intelligence Systems, CCIS 2012, Hangzhou, China, October 30 - November 1, 2012* (2012), IEEE, pp. 176–180. 5

[SLFC19] STETS J. D., LI Z., FRISVAD J. R., CHANDRAKER M.: Single-shot analysis of refractive shape using convolutional neural networks. In *IEEE Winter Conference on Applications of Computer Vision, WACV 2019, Waikoloa Village, HI, USA, January 7-11, 2019* (2019), IEEE, pp. 995–1003. 6

[Sta99] STAM J.: Stable fluids. In *Proceedings of the 26th Annual Conference on Computer Graphics and Interactive Techniques, SIGGRAPH 1999, Los Angeles, CA, USA, August 8-13, 1999* (1999), Waggenspack W. N., (Ed.), ACM, pp. 121–128. 1

[TKPR09] THÜREY N., KEISER R., PAULY M., RÜDE U.: Detail-preserving fluid control. *Graph. Model. 71*, 6 (2009), 221–228. 3

[TL19] TAKAHASHI T., LIN M. C.: Video-guided real-to-virtual parameter transfer for viscous fluids. *ACM Trans. Graph. 38*, 6 (2019), 237:1–237:12. 1

[TLY20] THAPA S., LI N., YE J.: Dynamic fluid surface reconstruction using deep neural network. In *2020 IEEE/CVF Conference on Computer Vision and Pattern Recognition, CVPR 2020, Seattle, WA, USA, June 13-19, 2020* (2020), IEEE, pp. 21–30. 1

[TS94] TSAI P., SHAH M.: Shape from shading using linear approximation. *Image Vis. Comput. 12*, 8 (1994), 487–498. 1

[TZG*18] TEWARI A., ZOLLHÖFER M., GARRIDO P., BERNARD F., KIM H., PÉREZ P., THEOBALT C.: Self-supervised multi-level face model learning for monocular reconstruction at over 250 hz. In *2018 IEEE Conference on Computer Vision and Pattern Recognition, CVPR 2018, Salt Lake City, UT, USA, June 18-22, 2018* (2018), IEEE Computer Society, pp. 2549–2559. 1

[WLZ*09] WANG H., LIAO M., ZHANG Q., YANG R., TURK G.: Physically guided liquid surface modeling from videos. *ACM Trans. Graph. 28*, 3 (2009), 90. 1

[WYZ*17] WANG D., YAN W., ZHU T., XIE Y., SONG H., HU X.: An adaptive correction algorithm for non-uniform illumination panoramic images based on the improved bilateral gamma function. In *2017 International Conference on Digital Image Computing: Techniques and Applications (DICTA)* (2017), pp. 1–6. 5

[ZTCS99] ZHANG R., TSAI P., CRYER J. E., SHAH M.: Shape from shading: A survey. *IEEE Trans. Pattern Anal. Mach. Intell. 21*, 8 (1999), 690–706. 1